NASA TECHNICAL NOTE

NASA TN D-7341

NASA TN D-7341

FLOW THROUGH A WIRE-FORM TRANSPIRATION-COOLED VANE

by Albert Kaufman

Lewis Research Center

Cleveland, Ohio 44135

NATIONAL AERONAUTICS AND SPACE ADMINISTRATION • WASHINGTON, D. C. • JUNE 1973

1. Report No.	2. Government Accession No.	3. Recipient's Catalog No.
NASA TN D-7341		

4. Title and Subtitle	5. Report Date
FLOW THROUGH A WIRE-FORM TRANSPIRATION-COOLED VANE	June 1973
	6. Performing Organization Code

7. Author(s)	8. Performing Organization Report No.
Albert Kaufman	E-7385
	10. Work Unit No.
9. Performing Organization Name and Address	501-24
Lewis Research Center National Aeronautics and Space Administration Cleveland, Ohio 44135	11. Contract or Grant No.
	13. Type of Report and Period Covered
12. Sponsoring Agency Name and Address	Technical Note
National Aeronautics and Space Administration Washington, D.C. 20546	14. Sponsoring Agency Code

15. Supplementary Notes

16. Abstract

Results of recent research at the NASA Lewis Research Center to develop techniques for analyzing coolant flow in transpiration-cooled vanes are summarized. Flow characteristics of the wire-form porous material are correlated, and the effects on the flow characteristics of oxidation, coolant temperature, gas crossflow, and airfoil curvature are evaluated. An analytical method is presented for predicting coolant flows and pressures in a strut-supported vane.

17. Key Words (Suggested by Author(s))

Turbine cooling
Transpiration cooling
Fluid flow
Aircraft propulsion
Oxidation

18. Distribution Statement

Unclassified - unlimited

19. Security Classif. (of this report)	20. Security Classif. (of this page)	21. No. of Pages	22. Price*
Unclassified	Unclassified	26	$3.00

* For sale by the National Technical Information Service, Springfield, Virginia 22151

FLOW THROUGH A WIRE-FORM TRANSPIRATION-COOLED VANE

by Albert Kaufman

Lewis Research Center

SUMMARY

Results of a number of programs at the NASA Lewis Research Center to develop techniques for predicting coolant flow and pressure distributions in wire-form transpiration-cooled vanes are reviewed and integrated. These studies include methods for determining flow characteristics of the porous material and the effects of material curvature, coolant temperature, and external gas flow on the flow characteristics. A method for predicting the effects of oxidation in reducing flow through transpiration-cooled walls and the development of more oxidation-resistant porous materials are described. Finally, an analytical procedure is presented for predicting coolant flow and pressure distributions and discharge airflows in a strut-supported transpiration-cooled vane.

INTRODUCTION

The NASA Lewis Research Center has undertaken a series of studies to develop methods for predicting coolant flow and pressure distributions in wire-form transpiration-cooled vanes designed for advanced airbreathing engines. These studies are discussed in references 1 to 5. It is the purpose of this report to review the principal results of these investigations in order to present a more integrated and convenient account to the reader than he would have if he read all these references separately.

The porous material studied under this program was a wound wire-form material called Poroloy. Because of its ease of fabrication and well-ordered structure, Poroloy has been a prime candidate for consideration in transpiration cooling of hot turbine components in turbojet engines.

A knowledge of the flow characteristics of the porous skin is a prerequisite to designing a transpiration-cooled vane. In reference 1, the flow resistances for a wide range of Poroloy geometries are correlated with the absolute filtration ratings of these geometries and with the flow rates at standard conditions by which the Poroloy is speci-

fied and ordered. Effects on the flow characteristics of specimen curvature and air temperature up to 722 K (844° F) are also discussed in reference 1.

One of the major problems in the design and utilization of transpiration-cooled vanes for airbreathing engines has been the susceptibility of the small pores to flow restriction because of oxidation. Once significant oxidation starts, the metal temperature rises and, for most wire alloys, further accelerates the oxidation and flow restriction process. In reference 2, a method is presented for predicting the flow reduction in Poroloy material from oxidation by using only oxidation data from wire samples. Although this would enable a designer to determine the approximate flow rate transpiring through the porous skin at any time, he would still be faced with the difficult situation of having to design a vane with flow resistances which vary with time.

In order to overcome these oxidation problems, an NASA contractor investigated available oxidation-resistant alloys for use in transpiration cooling. The contractor was successful in developing fabrication procedures that permitted several of the most promising oxidation-resistant alloys to be fabricated into Poroloy. These highly oxidation-resistant forms of Poroloy permitted a significant increase in the useful temperature range for Poroloy-type transpiration-cooled materials. The details of this program are reported in reference 3.

In reference 4, an analytical method is presented for predicting airflow rates and pressure distributions in the coolant distribution passages of a strut-supported vane and the discharge flow rates from the porous skin. The validity of this method was verified by comparing analytical results with experimental data obtained from cold-flow tests of a vane in a bench-type flow facility.

In these cold-flow tests, the vane was in a static, ambient environment, whereas, in an engine, gas would be flowing along the outside airfoil surfaces. Therefore, there was still some question as to how well the analytical model of reference 4 actually represented conditions during engine operation. In order to settle this question, an experiment was conducted wherein gas, with free-stream Mach numbers up to 0.46, was flowed along the discharge surface of a flat Poroloy specimen to determine if the external flow affected the flow characteristics. The results from this experiment are discussed in reference 5.

In order to present the results of references 1 to 5 in the most logical manner, the chronological order in which these references were published has been disregarded. Since the intent of this report is to review only the significant features and conclusions of references 1 to 5, discussion of the test apparatus and procedures, as well as sources or derivations of equations, is kept to a minimum. The reader is referred to the applicable reference for these details.

DISCUSSION

Flow Characteristics

Correlation of flow resistances. - The surface appearance of a typical Poroloy material used for transpiration cooling is shown in figure 1. In order to design a transpiration-cooled vane, the flow characteristics of the particular Poroloy configuration must be known. If the designer is to do a conceptual study, with no particular configuration in mind or available for flow testing, he must be supplied with some unique relation between the flow resistances and some parameter which can be used to specify the Poroloy structure.

Two parameters which have been used extensively for specifying wire-form porous materials are the mass flow rate per unit area under standard conditions G_s and the absolute filtration rating AFR. (Symbols are defined in the appendix.) The latter is equivalent to the diameter of the largest glass bead, in a slurry of beads, which will flow through the porous material. A correlation between G_s and AFR, based upon a limited number of slurry tests, is presented in reference 2.

The standard equation that has been used for calculating fluid flow through a porous media is the so-called Green equation, which can be written as

$$\frac{\left(P_U^2 - P_D^2\right)g}{\tau\mu(2RTG)} = \alpha + \beta\left(\frac{G}{\mu}\right) \tag{1}$$

where α is a viscous resistance coefficient defining the viscous shear losses, and β is an inertial resistance coefficient defining the losses in the tortuous internal passages. The resistance coefficients for a particular Poroloy configuration can be obtained by measuring the transpiring airflow rates for different combinations of upstream and downstream pressures. If these flow data are plotted in terms of the parameter on the left side of equation (1) against G/μ, all the data should fall on a straight line with an intercept equal to α and a slope equal to β.

Flow resistance coefficients for different Poroloy configurations with thicknesses of about 0.061 centimeter (0.024 in.) were determined from room-temperature flow tests of flat specimens; these tests were conducted by NASA and a contractor (refs. 1 and 6, respectively). The 0.061-centimeter (0.024-in.) wall thickness is commonly used for wire cloth airfoil shells for transpiration cooling because it is the minimum practicable thickness which can withstand impact damage from foreign objects in an engine. All subsequent results presented in this report also apply for approximately the same Poroloy wall thickness.

The viscous- and inertial-resistance coefficients from references 1 and 6 are correlated as logarithmic functions of G_s in figure 2. Generally, the data fall on a straight line with the exception of some of the reference 6 data at high flow rates in figure 2(a). Reference 1 data for similar standard flow rates did not exhibit the sharp drop from the straight line and the scatter shown by the reference 6 data in figure 2(a). The following exponential equations can be obtained from the straight-line plots of figure 2:

$$\alpha = 39.7 \times A \times 10^8 (C \times G_s \times 10^3)^{-1.29} \tag{2}$$

$$\beta = 35.6 \times B \times 10^5 (C \times G_s \times 10^3)^{-1.61} \tag{3}$$

where A is 1550, B is 39.4, and C is 703 for SI units and all three constants are unity for U.S. customary units. Based on the absolute filtration rating, where $AFR = 7.5\ G_s$ for G_s in SI units and $AFR = 5357\ G_s$ for G_s in U.S. customary units, these flow resistance equations become

$$\alpha = 350 \times A \times 10^8 (AFR)^{-1.29} \tag{4}$$

$$\beta = 540 \times B \times 10^5 (AFR)^{-1.61} \tag{5}$$

Equations (2) to (5) permit the calculation of flow rates for any design condition without having to obtain samples of the porous material beforehand and resorting to flow tests to determine the flow resistances. The equations also enable a designer to evaluate various porous configurations by means of a paper study before selecting a specific configuration.

Effect of curvature. - One of the most important and difficult regions of a vane to cool is the leading edge. The possibility exists that the sharp curvature in the initially flat Poroloy sheet could result in distortion of the porous structure and a change in the flow characteristics. The effects of curvature on the Poroloy material were investigated (ref. 1) by flow testing curved specimens which were progressively deformed so that their radii decreased from 1.27 to 0.25 centimeter (0.5 to 0.1 in.). Three curved specimens were tested in this manner in order to evaluate the reproducibility of the results. Contoured plastic tubing was used to collect the airflow discharging from the curved surface. The results of these tests are shown in figure 3, where the flow characteristics are nondimensionalized with respect to those determined for the cylinder with an initial radius of 1.27 centimeters (0.5 in.). The high degree of data scatter in the flow resistances α and β in figures 3(a) and (b) is attributed to the difficulty of attaining perfect contact between the contoured probes and the Poroloy surfaces for the

high curvatures used. The small scatter shown in figure 3(c) would indicate that the flow rate is relatively insensitive to small measurement inaccuracies compared to the flow resistance coefficients. In general, the data points in figure 3 scatter around unity; therefore, it can be concluded that if any effects of curvature on the flow characteristics exist, they are too minor to be of concern to a designer.

Effect of hot airflow. - In reference 6, the effects on the flow resistances of elevated temperatures were investigated by flowing 422 K (300° F) air through Poroloy specimens; based on these tests, the authors concluded that no significant effect existed. In reference 1, this investigation was extended by transpiring 644 to 722 K (700° to 840° F) air through Poroloy. The results of these tests are presented in figure 4, where the flow characteristics are nondimensionalized with respect to room-temperature flow results. As in figure 3, the data points tend to scatter around unity with the flow resistances showing greater scatter than the standard flow rates. These results tend to confirm the tentative conclusion reached in reference 6, that flow characteristics determined from cold-flow tests are applicable to hot-airflow conditions.

Effect of external gas flow. - In an aircraft gas turbine, a transpiration-cooled vane is in a dynamic environment with gas flowing through the channels between adjacent vanes and mixing with the coolant discharging from the airfoil surface. Experimental studies of flow through perforated plates by other investigators indicated that, when the plates were subjected to crossflow, the normal flow for a given pressure drop was reduced. Although the transpiration-cooling material is far removed from a perforated plate, there was some concern that the flow characteristics of the material in an engine environment could be substantially different from those obtained from flow tests conducted in a static environment. In order to settle this question, an experiment (ref. 5) was conducted in which a transpiration flow specimen was subjected to external gas flow along the discharge surface at free-stream Mach numbers from 0 to 0.46. The flow results from these tests are correlated in figure 5 in terms of the pressure and flow parameters of equation (1). A straight-line curve fit was drawn through the zero Mach number data. The data points representing external gas flow with free-stream Mach numbers from 0.40 to 0.46 scatter on both sides of this base line. These results demonstrate that the gas-stream external flow up to a Mach number of 0.46 does not affect the Poroloy flow characteristics as determined from tests in a static environment or from the correlations of equations (2) to (5).

Oxidation Characteristics

Flow restriction effects. - In order to obtain the high cooling effectiveness associated with transpiration cooling, very small, closely spaced pores are required. Un-

fortunately, in advanced air-breathing engines the porous material can be subjected to metal temperatures from 1144 to 1255 K (1600° to 1800° F); at these temperatures oxide tends to build up around the small pores and causes progressive flow restriction with an accompanying rise in metal temperature and accelerated oxidation.

A method is presented in reference 2 for calculating the flow reduction in Poroloy with time; this method is based on experimental oxidation data from tests on wire samples of the same wire diameter and alloy from which the Poroloy material is fabricated. In determining the oxide growth on the wires, the diameter changes are determined for both cyclic and steady-state oxidation conditions. The increase in wire diameter is averaged for the two oxidation conditions; the rationale for this is that cyclic oxidation from engine starting and stopping would force much of the oxide built up near the airfoil discharge surface to spall off, but would not remove any oxide formation in the interior of the wall. The analysis is based on the assumption that the small pores act as capillaries and, therefore, the flow rate is proportional to the fourth power of the pore diameter or the absolute filtration rating of the Poroloy configuration. Thus, the percent flow reduction can be represented by $\left\{1 - \left[(d - t)/d\right]^4\right\} \times 100$, where d is the initial pore diameter as defined by the absolute filtration rating and t is the increase in wire diameter at the temperature and exposure time under consideration.

Measured wire diameter changes caused by both cyclic and steady-state oxidation at temperatures from 1033 to 1367 K (1400° to 2000° F) and exposure times up to 600 hours for four alloys (N 155, DH 242, thoria-dispersion-strengthened nickel-chromium (TD-NiCr), and Hastelloy X) which were being used or considered for transpiration cooling are reported in reference 7. Flow test results for oxidized Poroloy specimens made from some of these alloys and some results of bead filtration tests (ref. 1) established the relation $AFR = 7.5\ G_s$, where G_s is in kilograms per second per square meter, or $AFR = 5357\ G_s$, where G_s is in pounds per second per square inch, for Poroloy geometries in the range of interest for transpiration cooling.

In figures 6(a) and (b), oxidation data at 1255 K (1800° F) are compared to predicted flow reductions for Poroloy fabricated from TD-NiCr and DH 242 wire. A similar comparison is made in figure 6(c) by using oxidation data from reference 6 on Hastelloy X Poroloy at metal temperatures from 1033 to 1367 K (1400° to 2000° F). All the flow tests used to determine oxidation effects were conducted under the same conditions as those used to measure the standard flow rate G_s. These comparisons demonstrate generally good agreement between data and predictions; the only serious discrepancy shown is in figure 6(c) for Hastelloy X at 1033 K (1400° F).

Development of oxidation-resistant material. - Until very recently, transpiration cooling was limited to maximum metal temperatures of the order of 1144 K (1600° F) because of the oxidation problem. The magnitude of this problem can be judged from figure 6(c), where the Hastelloy X Poroloy shows a flow reduction of about 80 percent

after 600 hours of exposure at 1144 K (1600° F). Although the flow reduction can be estimated by means of the capillary flow model discussed in the previous section, the design of a transpiration-cooled vane with flow characteristics which vary with time is an extremely difficult problem.

In order to overcome the oxidation limitations on transpiration cooling, a program was undertaken to develop Poroloy materials with improved oxidation resistance and stability. As a result of this program, a process was developed for fabricating oxidation-resistant Poroloy from iron-chromium-aluminum alloys, which are difficult to diffusion bond. The most promising of these alloys was GE 1541 (15 percent chromium - 4 percent aluminum - 1 percent yttrium - balance iron). Details of the fabrication process are described in reference 3.

Based on data presented in reference 3, the oxidation resistance of GE 1541 Poroloy at 1367 K (2000° F) is compared in figure 7 to that of DH 242 at 1200 K (1700° F) and to that of another iron-base material, H 875, at 1367 K (2000° F). At the time this study was initiated, DH 242 was probably the most favored material for transpiration cooling utilizing wire-cloth airfoils. Figure 7 demonstrates that the GE 1541 and H 875 Poroloy materials represent an advance of over 167 K (300° F) in the state of the art of transpiration cooling. Another important feature of the GE 1541 oxidation characteristics is that no further oxidation occurs after an initial flow reduction in the first few hours of exposure. This means that, by preoxidizing GE 1541 Poroloy in an oven for this initial period, stable flow characteristics can be attained.

Prediction of Vane Pressure and Flow Distributions

An analytical method for predicting coolant flows and pressures in the coolant distribution passages of a strut-supported vane and the discharge flow from the porous skin is presented in reference 4. The validity of this method was established by comparing predicted flows and pressures with experimental results obtained from cold-flow tests on a transpiration-cooled vane.

Vane description. - The research vane, shown in figure 8, was designed for NASA by a contractor. This vane consisted of a cast Udimet 700 strut with fluted coolant passages and a Poroloy airfoil shell which was electron-beam welded to the strut. Cooling air supplied to the vane through a tube attached to the tip shroud first impinged on a baffle before entering a plenum chamber in the shroud. The coolant was then distributed through metering orifices to the 10 spanwise coolant passages. As the coolant flowed through these passages, it was progressively discharged through the porous airfoil shell.

Analytical model. - The flow model which was used to predict the coolant flow and pressure distribution is shown in figure 9. The air discharging from the orifice into

the passage suffers an expansion loss because of the abrupt enlargement of the flow area. In this portion of the passage, designated region A and estimated to extend for a distance of seven passage hydraulic diameters, the static pressure is assumed to vary linearly from the orifice exit (station 2) to the flow reattachment point (station 3). Completely recovered flow exists in region B, which consists of the remainder of the passage. An exception to this model was the trailing-edge passage, where the orifice and passage areas were equal; in this case, obviously no expansion region existed.

Analytical procedure. - The following procedure, which was developed in reference 4, is used to compute the flow and coolant distributions based on the flow model of figure 9 and orifice discharge data from reference 8:

(1) An orifice discharge coefficient is determined from experimental data for thick-plate orifices given in reference 8. If these data are sensitive to Reynolds number, it may be necessary to correlate the data in terms of Reynolds number and solve for the discharge coefficient by iteration.

(2) Initially, an orifice flow rate is assumed.

(3) The static pressure at the orifice exit (station 2) is calculated from the orifice discharge coefficient. The orifice discharge coefficient is defined as

$$C_d = \frac{\dot{w}_o}{P_2 V_2 A_0} \tag{6}$$

where

$$V_2 = \sqrt{\frac{2\gamma g R T'}{\gamma - 1}\left[1 - \left(\frac{P_2}{P_1'}\right)^{\gamma - 1/\gamma}\right]} \tag{7}$$

and

$$\rho_2 = \frac{P_2}{RT'}\left(\frac{P_1'}{P_2}\right)^{\gamma - 1/\gamma} \tag{8}$$

(4) The total pressure in the orifice is calculated from the measured plenum pressure and from a compressible flow solution for an abrupt contraction. This solution can be stated in terms of the ratio of orifice to plenum total pressure as

$$\frac{P_o'}{P_1'} = \left[\frac{P_2}{P_o'}(-0.587\,\beta_{in}^2 + 0.0399\,\beta_{in} + 0.572) + (0.587\,\beta_{in}^2 - 0.0399\,\beta_{in} + 0.428)\right] \tag{9}$$

where

$$\beta_{in} = \frac{D_{h,o}}{D_{h,1}} \tag{10}$$

Equation (8) is applicable where β_{in} is less than 0.3 and P_2/P'_o is greater than 0.75, which was true for all the passages in the vane design. The plenum pressure is the only pressure measurement which is required for the analysis. Because of the presence of the inlet baffle, the total and static pressures at station 1 were identical in the research vane.

(5) The total pressure at the reattachment point (station 3) is calculated from a compressible-flow solution for an abrupt expansion. The ratio of the total pressure at the reattachment point to that at the orifice is

$$\frac{P'_3}{P'_o} = 1 - \left(1 - \frac{P_o}{P'_o}\right)\left(1 - \beta_{out}^2\right)^2 \tag{11}$$

where

$$\beta_{out} = \sqrt{\frac{A_o}{A_p}} \tag{12}$$

(6) The flow distribution in region A can now be determined by using the static pressure at station 2 (from step (3)); an initial estimate of the static pressure at station 3; the flow discharge equation for a porous media, which is defined in equation (6); the flow resistances for the Poroloy material from figure 2; and the assumption of a linear rise in static pressure in region A.

(7) An improved estimate of static pressure at the reattachment point can now be computed from the calculated flow rate at that station.

(8) Iteration is continued until convergence is obtained between the static pressures at station 3 from steps (6) and (7).

(9) The flow and pressure distributions in region B are obtained from equation (6) and from a one-dimensional compressible-flow equation for a passage with flow ejection. This equation is given here in finite difference form for each increment of span distance ΔX into which the passage is divided:

$$\Delta P = \left[\frac{-\left(\frac{RT}{gP}\right)\left(\frac{\dot{w}}{A_p}\right)\left(\frac{\Delta \dot{w}}{A_p \Delta X}\right) - \left(\frac{\dot{w}}{A_p}\right)^2 \left(\frac{R}{gP}\right)\left(\frac{fT}{2D_{h,p}} + \frac{\Delta T}{\Delta X}\right)}{1 - \left(\frac{\dot{w}}{A_p}\right)^2 \left(\frac{RT}{gP^2}\right)} \right] \Delta X \tag{13}$$

where for laminar flow

$$f = \frac{64}{(Re)_p} \tag{14}$$

and for turbulent flow

$$f = \frac{0.186}{(Re)_p^{0.2}} \tag{15}$$

(10) Steps (1) to (9) are repeated until the flow rate at the end of the passage (station 4) becomes essentially zero.

Comparison of analytical and experimental results. - The analytical procedure was verified by comparing flow and pressure predictions with experimental results for cold-flow tests of an instrumented vane. This vane contained static-pressure taps at the hub, midspan, and tip of every passage; in addition, discharge airflows were measured by means of contoured probes at seven span positions along the airfoil for each passage. Predicted and measured results for a vane inlet flow of 33.2 grams per second (0.0731 lb/sec) are compared in figure 10 for the flow distributions in the coolant passages, in figure 11 for the static-pressure distributions in the coolant passages, and in figure 12 for the discharge flow rates through the Poroloy airfoil. The experimental data of figures 10 and 11 show very good agreement with the predicted flow and pressure distributions in the passages. Somewhat larger discrepancies are found in figure 12 between the measured and predicted discharge flow rates; however, agreement is still good, considering the fact that the discharge flow rates for a span increment are small values and considering the possible fabrication errors and inaccuracies in pressure and flow measurements.

CONCLUDING REMARKS

Although the results presented in this report are for one specific transpiration-

cooling material (Poroloy), the general techniques used are applicable to most porous materials. In reference 6, it is demonstrated that Lamilloy, a porous material made by photoetching and diffusion bonding laminates, obeys the Green equation for flow through a porous medium. In reference 1, the Lamilloy flow characteristics are successfully correlated with geometrical parameters. Not all porous materials require an internal strut for support; sometimes stiffening laminates along the inside surface of the airfoil are sufficient to enable the vane to withstand gas bending and thermal stresses. When a strut support is not used, the internal cavity of the vane is merely a plenum, and the flow and pressure computations are greatly simplified compared to the analytical procedure of reference 4.

The major problem in applying the techniques derived in references 1 to 5 in designing a transpiration-cooled vane for an actual engine environment is in determining the external pressure distribution around the airfoil. Attempts have been made at the NASA Lewis Research Center to calculate coolant flows through transpiration-cooled vanes tested in the high-temperature cascade described in reference 9. The calculations used an external static-pressure distribution which had been measured around a convection-cooled vane. These attempts have been successful in predicting the total vane inlet flow rates only for coolant- to gas-flow ratios under 0.05; the higher the flow rate above this level, the greater the error in the calculated inlet flow rate. These results are not surprising since one would expect that, the higher the vane flow rate, the more chance there would be for the discharge flow from the airfoil to disrupt the boundary layer and affect the external pressure distribution. Unfortunately, there exist neither analytical techniques nor sufficient aerodynamic data on transpiration cooling to analyze these effects.

CONCLUSIONS

This report has reviewed the results of a number of studies undertaken at the NASA Lewis Research Center to develop methods for predicting flow and pressure distributions in transpiration-cooled vanes. The main conclusions that are drawn from these studies are as follows:

1. The flow resistances of the Poroloy material are uniquely related to the standard flow rate and to the absolute filtration rating of the material. Either of these parameters can be used to determine the flow resistances from correlations which are presented in this report.

2. The flow resistances are not affected by sharp curvatures such as exist at airfoil leading edges, by external gas flow along the airfoil surfaces, or by coolant temperatures up to 722 K (840° F).

3. Flow reductions caused by oxidation can be estimated from wire oxidation data, a capillary flow model, the absolute filtration rating of the porous material, and wire oxidation data.

4. Development of oxidation-resistant Poroloy from GE 1541 and H 875 alloys has extended the usable temperature range of the material by more than 167 K (300° F). Poroloy fabricated from GE 1541 exhibits very stable oxidation characteristics at 1367 K (2000° F) after the first few hours of exposure.

5. An analytical method has been developed by means of which the coolant flow rates and pressures in the coolant passages of a strut-supported vane and the discharge flow rates around the porous airfoil can be predicted with good accuracy.

Lewis Research Center,
National Aeronautics and Space Administration,
Cleveland, Ohio, April 13, 1973,
501-24.

APPENDIX - SYMBOLS

A	area or flow correlation coefficient
AFR	absolute filtration rating
B	flow correlation coefficient
C	flow correlation coefficient
C_d	orifice discharge coefficient
D_h	hydraulic diameter
d	initial pore diameter
f	D'Arcy-Weisbach friction factor
G	mass flow rate per unit area
G_s	standard flow rate per unit area under standard conditions
G'_s	standard flow rate per unit area under standard conditions with P_U and P_D determined at elevated temperatures
g	universal gravitational constant
l	span length of passage
P	static pressure
P'	total pressure
P_D	downstream static pressure
P_U	upstream static pressure
R	gas constant
Re	Reynolds number
T	static temperature
T'	total temperature
t	increase in wire diameter
V	velocity
$\dot{w}$	mass flow rate
$\Delta\dot{w}$	mass flow rate discharging through porous skin over span distance increment
x	span distance from orifice
Δx	span distance increment

α viscous-resistance coefficient determined at room temperature

α' viscous-resistance coefficient determined at elevated temperature

β inertial-resistance coefficient determined at room temperature

β' inertial-resistance coefficient determined at elevated temperature

β_{in} $D_{h,o}/D_{h,1}$

β_{out} $\sqrt{A_o/A_p}$

γ ratio of specific heats

μ viscosity

ρ density

τ porous material thickness

Subscripts:

o orifice

p passage

r with respect to radius r

s at standard conditions of $P_U = 17.0$ N/cm^2 (24.7 psia), $P_D = 10.1$ N/cm^2 (14.7 psia), and T = 294 K (70^o F)

1 plenum

2 orifice exit

3 reattachment point in passage

REFERENCES

1. Kaufman, Albert; and Richards, Hadley T.: Investigation of Flow Characteristics of Some Wire-Form and Laminate-Form Porous Materials. NASA TM X-2111, 1970.

2. Kaufman, Albert: Analytical Study of Flow Reduction Due to Oxidation of Wire-Form Porous Sheet for Transpiration Cooled Turbine Blades. NASA TN D-5001, 1969.

3. Madsen, Per; and Rusnak, Robert M.: Oxidation Resistant Porous Materials for Transpiration Cooled Vanes. NASA CR-1999, 1972.

4. Kaufman, Albert; Poferl, David J.; and Richards, Hadley T.: Coolant Pressure and Airflow Distribution in a Strut-Supported Transpiration-Cooled Vane for a Gas Turbine Engine. NASA TN D-6916, 1972.

5. Kaufman, Albert; Russell, Louis M.; and Poferl, David J.: Gas Crossflow Effects on Airflow Through a Wire-Form Transpiration-Cooling Material. NASA TM X-2687, 1972.

6. Anderson, R. D.; and Nealy, D. A.: Evaluation of Laminated Porous Material for High-Temperature Air-Cooled Turbine Blades. Rep. EDR-4968, General Motors Corp. (NASA CR-72281), Jan. 16, 1967.

7. Cole, Fred W.; Padden, James B.; and Spencer, Andrew R.: Oxidation Resistant Materials for Transpiration Cooled Gas Turbine Blades. Part Two: Wire Specimen Tests. NASA CR-1184, 1968.

8. Rohde, John E.; Richards, Hadley T.; and Metger, George W.: Discharge Coefficients for Thick Plate Orifices with Approach Flow Perpendicular and Inclined to the Orifice Axis. NASA TN D-5467, 1969.

9. Calvert, Howard F.; Cochran, Reeves P.; Dengler, Robert P.; Hickel, Robert O.; and Norris, James W.: Turbine Cooling Research Facility. NASA TM X-1927, 1970.

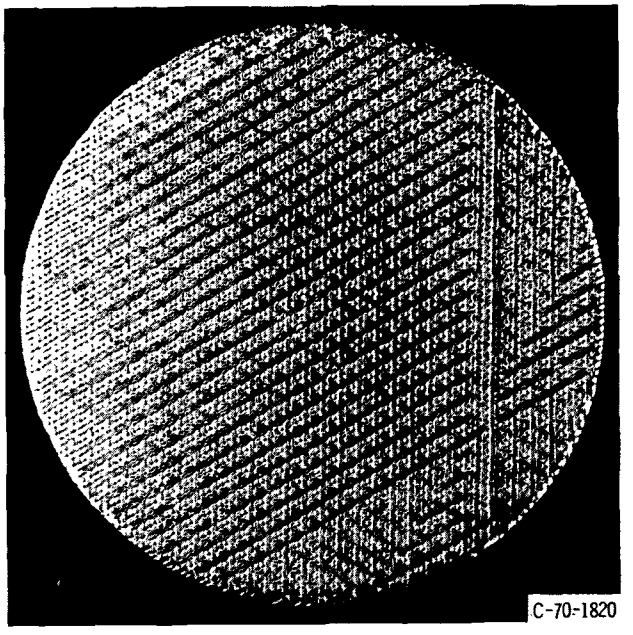

Figure 1. - Surface view of Poroloy wire-form transpiration-cooling material.

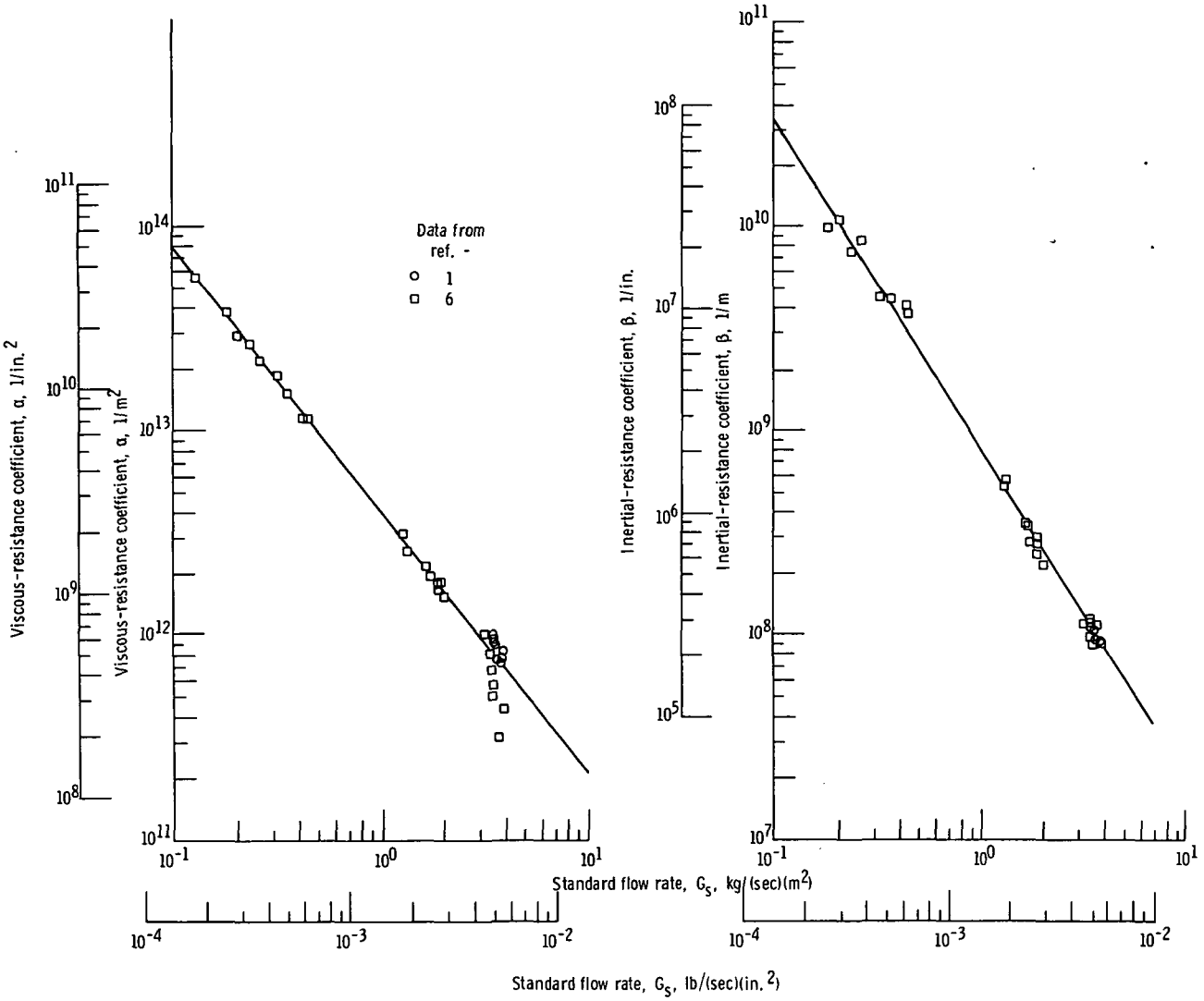

(a) Viscous-resistance-coefficient correlation.

(b) Inertial-resistance-coefficient correlation.

Figure 2. - Poroloy flow resistances as functions of standard flow rate. (From ref. 1.)

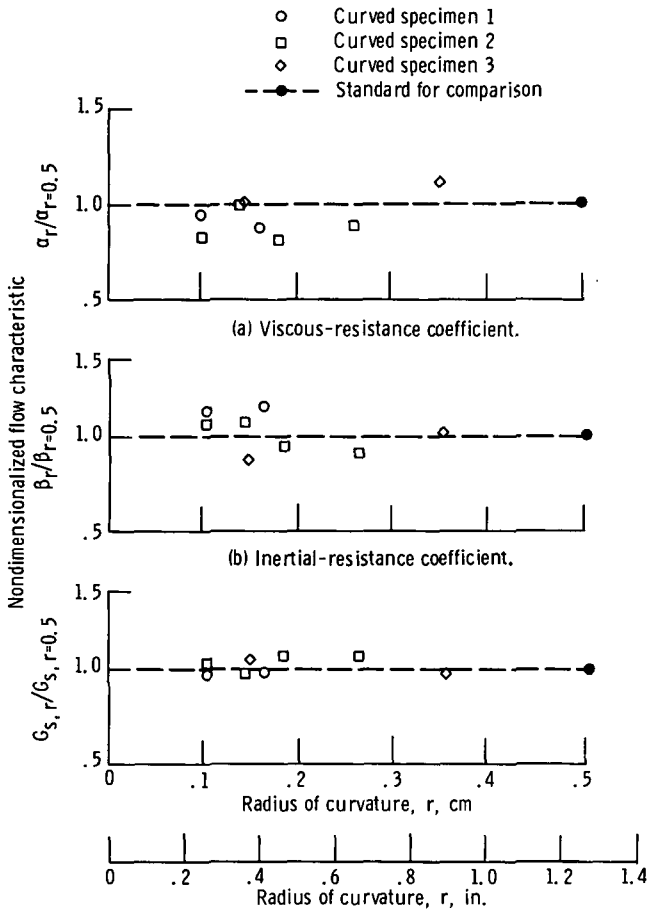

(a) Viscous-resistance coefficient.

(b) Inertial-resistance coefficient.

(c) Standard flow rate.

Figure 3. - Effect of Poroloy sheet radius of curvature on flow characteristics. (From ref. 1.)

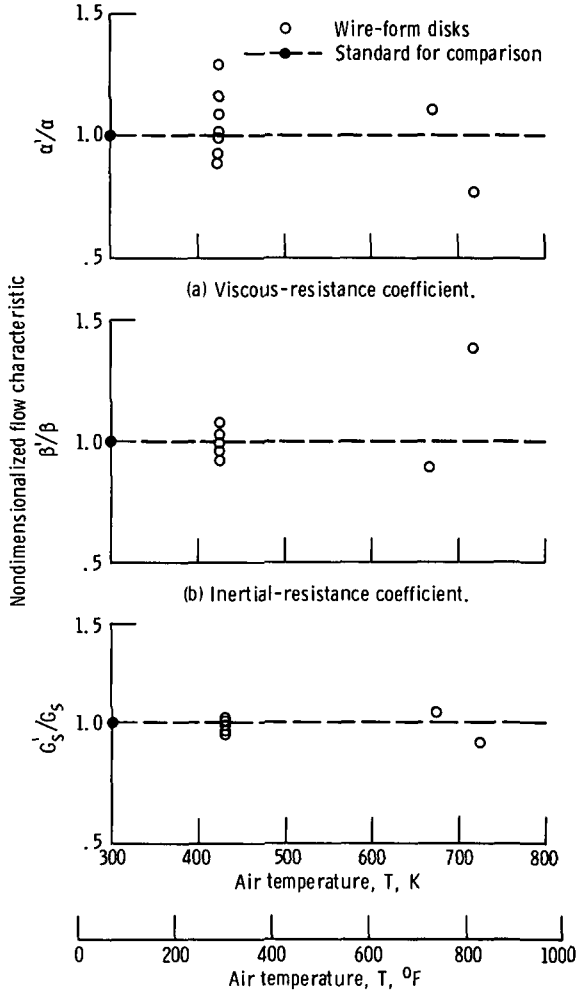

(a) Viscous-resistance coefficient.

(b) Inertial-resistance coefficient.

(c) Standard flow rate.

Figure 4. - Effect of air temperature on Poroloy flow characteristics. (From ref. 1.)

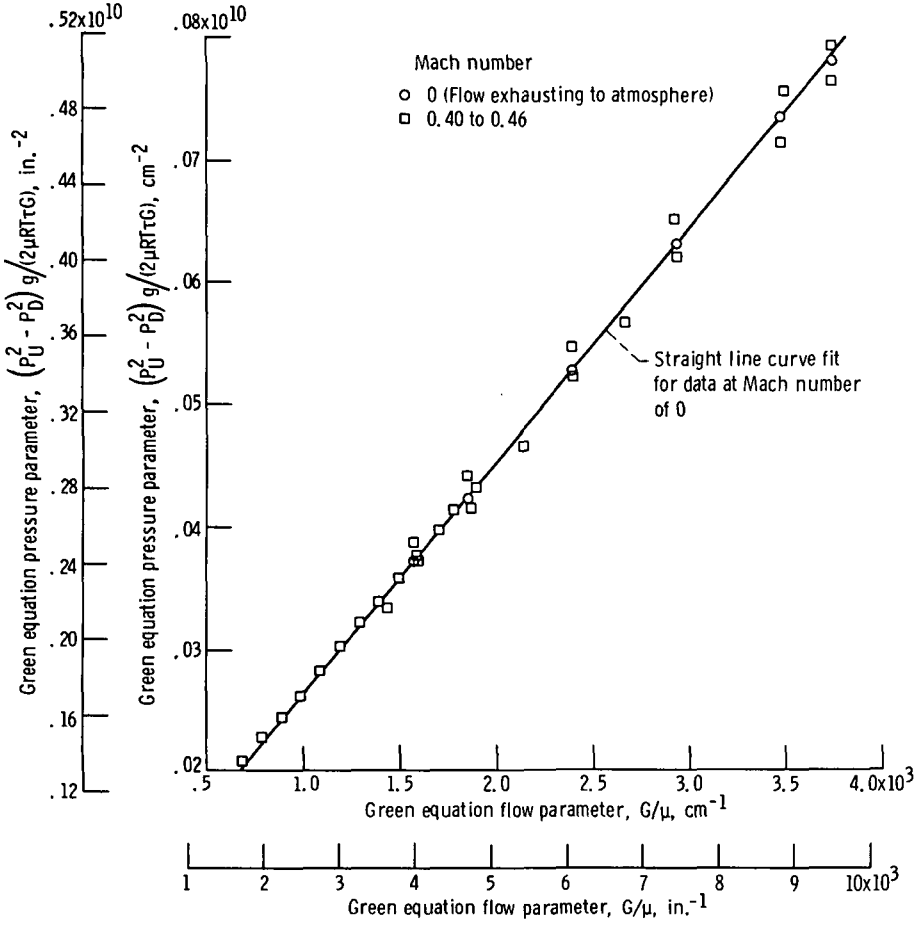

Figure 5. - Effect of external gas stream Mach numbers up to 0.46 on Poroloy specimen flow characteristics. (From ref. 5.)

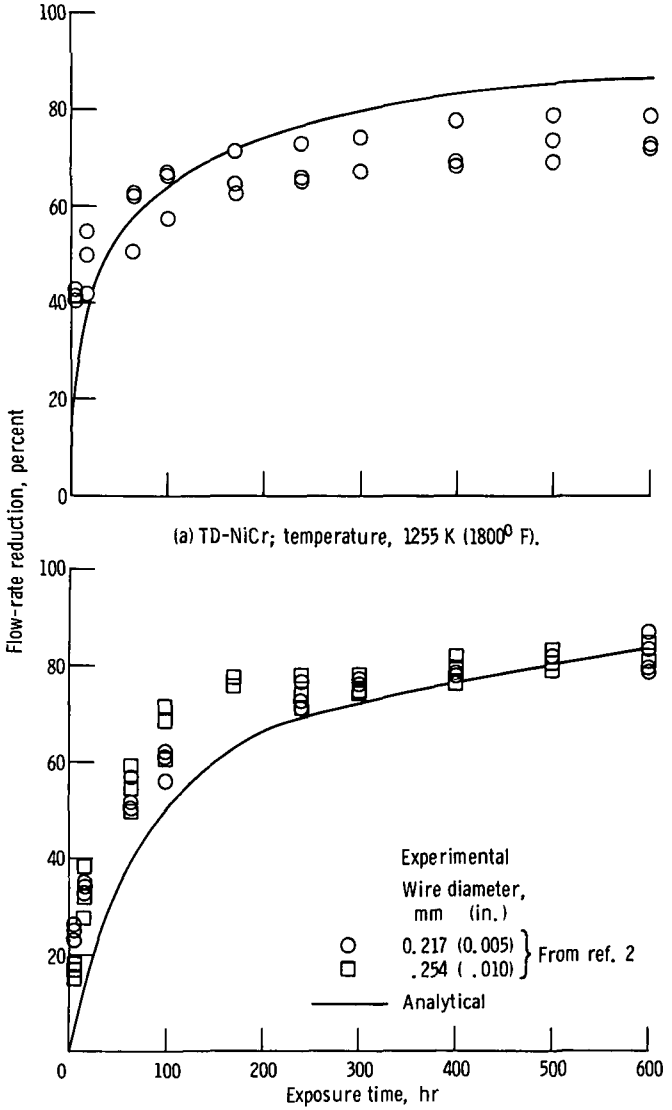

Figure 6. - Comparison of analytical predictions of flow-rate reduction due to oxidation exposure with oxidation test results for various Poroloy materials.

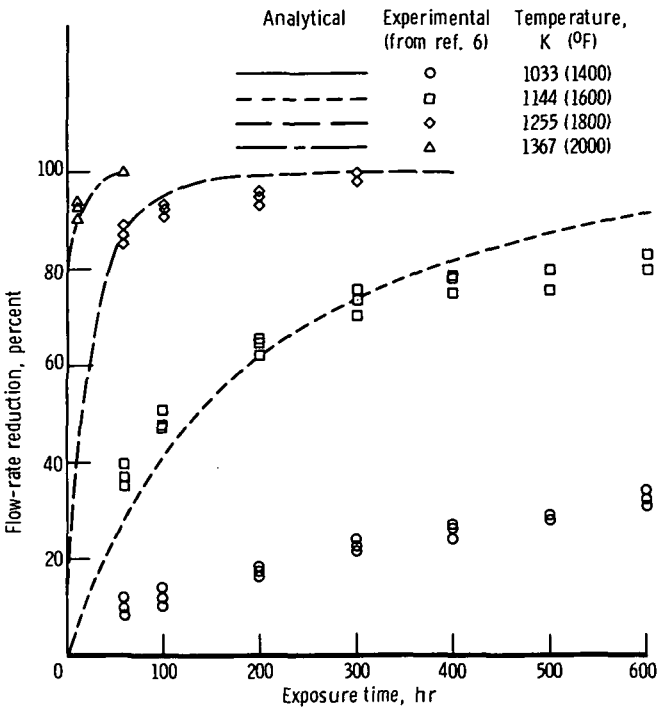

(c) Hasteloy X.

Figure 6. - Concluded.

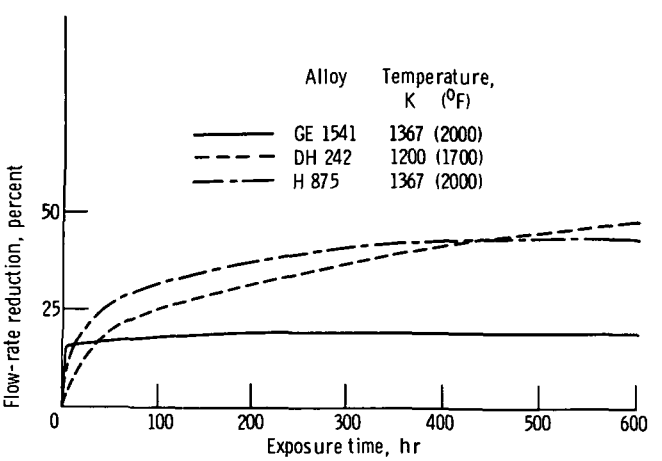

Figure 7. - Comparison of oxidation characteristics of Poroloy materials fabricated from DH 242, H 875, and GE 1541 alloys based on data presented in reference 3.

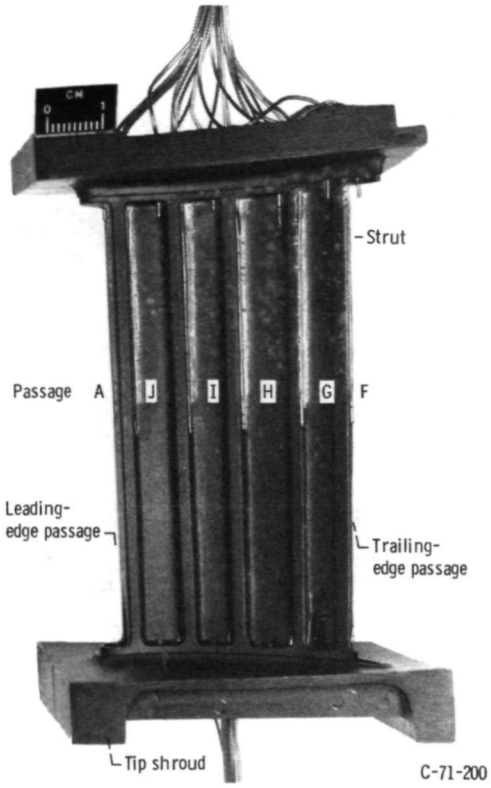

(a) Before porous shell was welded to strut - pressure side.

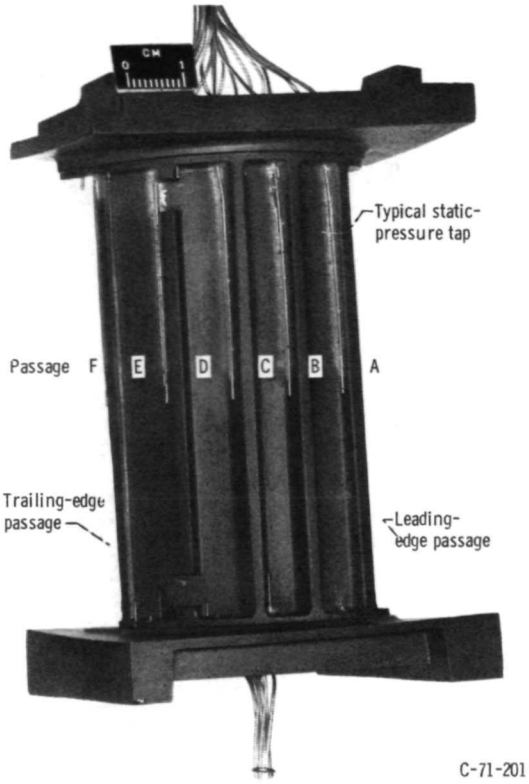

(b) Before porous shell was welded to strut - suction side.

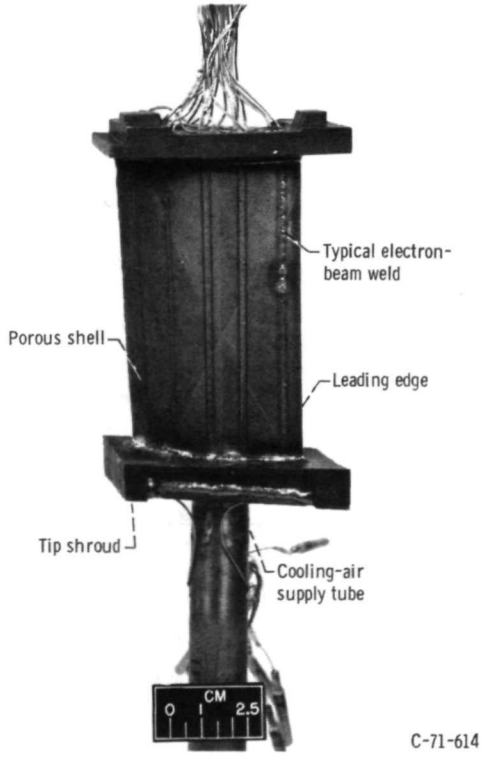

(c) After porous shell was welded to strut.

Figure 8. - Transpiration-cooled vane. (From ref. 4.)

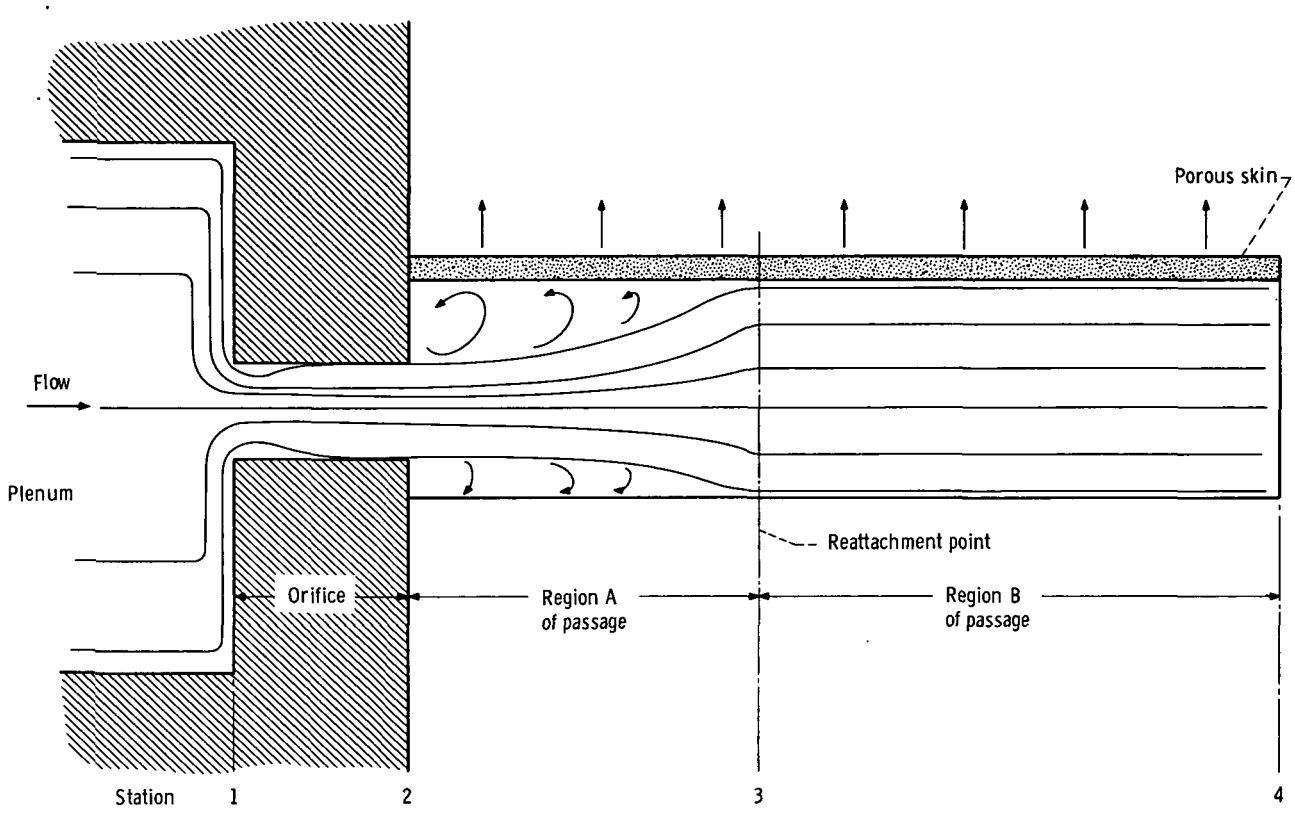

Figure 9. - Flow model of coolant passage. (From ref. 4.)

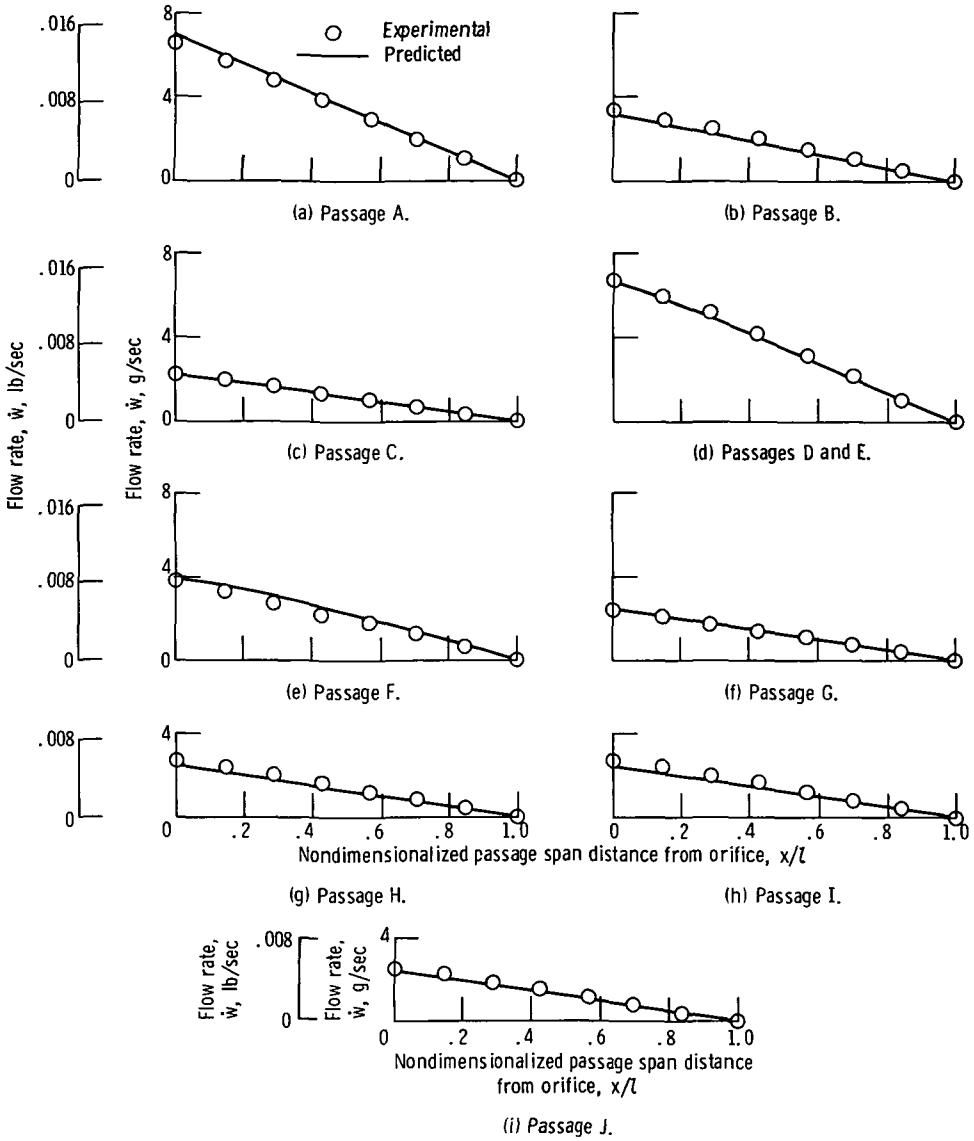

Figure 10. - Airflow distribution in vane coolant passages for inlet flow of 33.2 grams per second (0.0731 lb sec). (From ref. 4.)

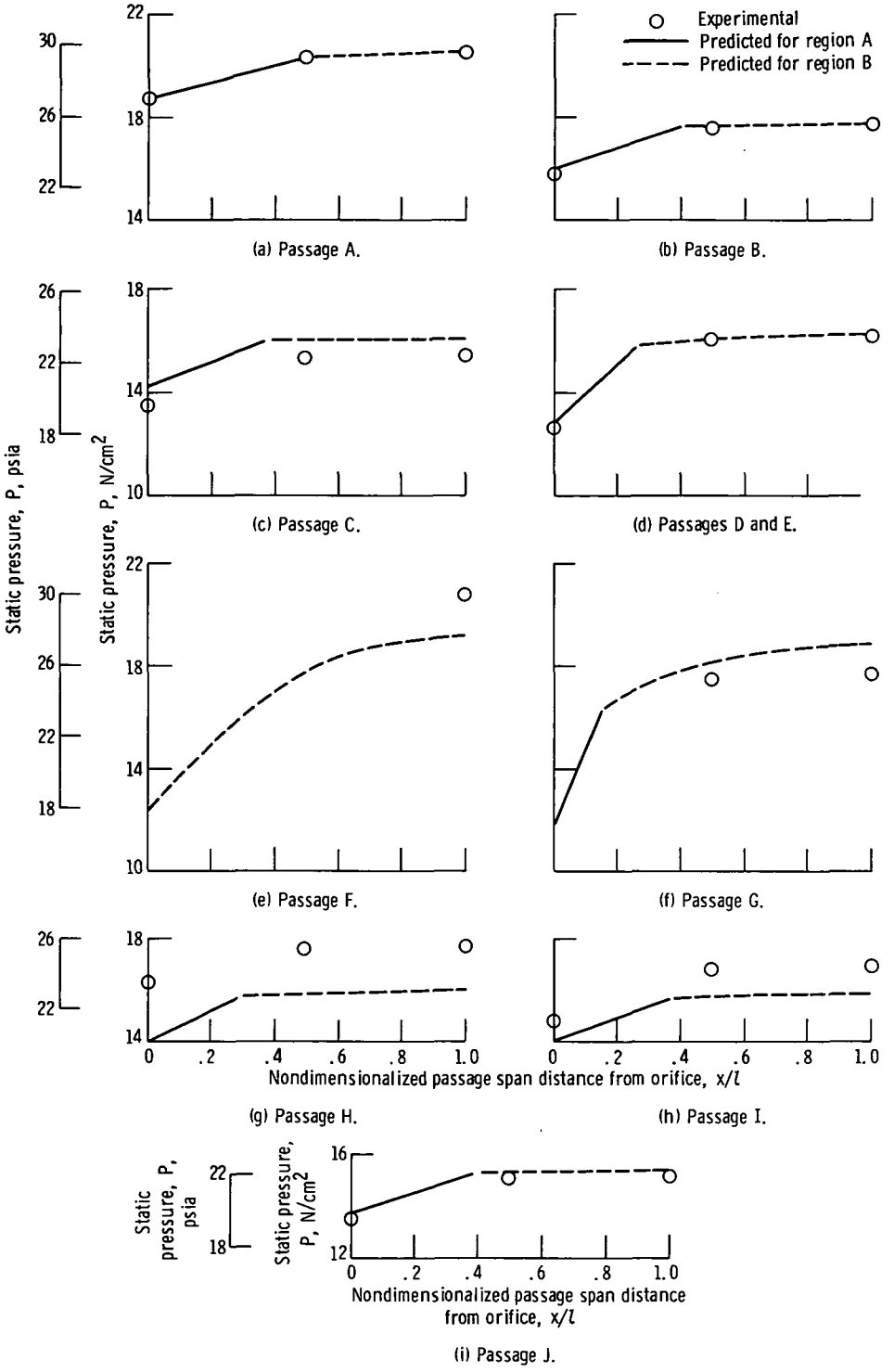

Figure 11. - Static-pressure distribution in vane coolant passages for inlet flow of 33.2 grams per second (0.0731 lb sec). (From ref. 4.)

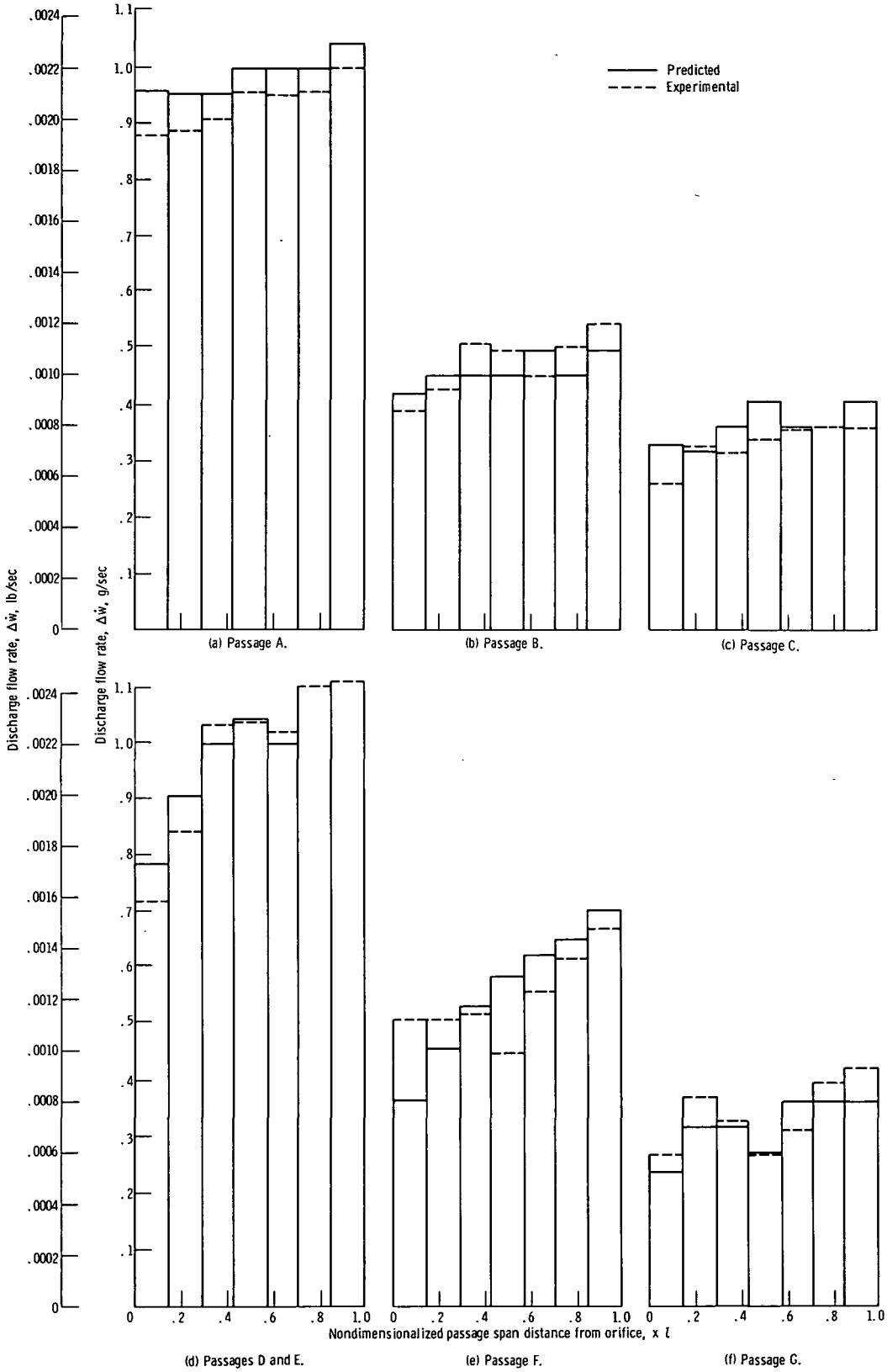

Figure 12. - Comparison of predicted and experimental discharge flow rates through porous shell of vane. (From ref. 4.)

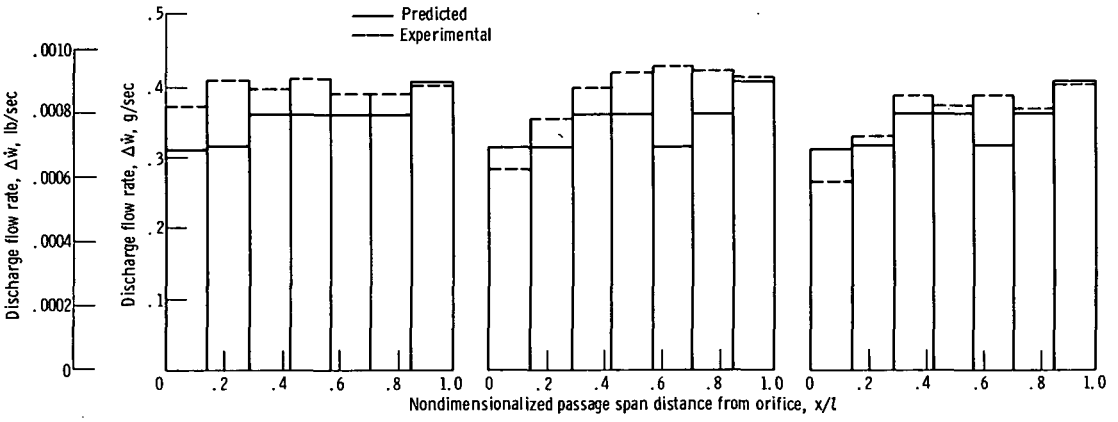

(g) Passage H. (h) Passage I. (i) Passage J.

Figure 12. - Concluded.

"The aeronautical and space activities of the United States shall be conducted so as to contribute . . . to the expansion of human knowledge of phenomena in the atmosphere and space. The Administration shall provide for the widest practicable and appropriate dissemination of information concerning its activities and the results thereof."

—NATIONAL AERONAUTICS AND SPACE ACT OF 1958

NASA SCIENTIFIC AND TECHNICAL PUBLICATIONS

TECHNICAL REPORTS: Scientific and technical information considered important, complete, and a lasting contribution to existing knowledge.

TECHNICAL NOTES: Information less broad in scope but nevertheless of importance as a contribution to existing knowledge.

TECHNICAL MEMORANDUMS: Information receiving limited distribution because of preliminary data, security classification, or other reasons.

CONTRACTOR REPORTS: Scientific and technical information generated under a NASA contract or grant and considered an important contribution to existing knowledge.

TECHNICAL TRANSLATIONS: Information published in a foreign language considered to merit NASA distribution in English.

SPECIAL PUBLICATIONS: Information derived from or of value to NASA activities. Publications include conference proceedings, monographs, data compilations, handbooks, sourcebooks, and special bibliographies.

TECHNOLOGY UTILIZATION PUBLICATIONS: Information on technology used by NASA that may be of particular interest in commercial and other non-aerospace applications. Publications include Tech Briefs, Technology Utilization Reports and Technology Surveys.

Details on the availability of these publications may be obtained from:

SCIENTIFIC AND TECHNICAL INFORMATION OFFICE

NATIONAL AERONAUTICS AND SPACE ADMINISTRATION

Washington, D.C. 20546